

Distributing Multipartite Entanglement over Noisy Quantum Networks

Luís Bugalho,^{1,2} Bruno C. Coutinho,² and Yasser Omar^{1,2}

¹*Instituto Superior Técnico, Universidade de Lisboa, Portugal*

²*Instituto de Telecomunicações, Physics of Information and Quantum Technologies Group, Portugal*

(Dated: March 1, 2025)

A quantum internet aims at harnessing networked quantum technologies, namely by distributing bipartite entanglement between distant nodes. However, multipartite entanglement between the nodes may empower the quantum internet for additional or better applications for communications, sensing, and computation. In this work, we present an algorithm for generating multipartite entanglement between different nodes of a quantum network with noisy quantum repeaters and imperfect quantum memories, where the links are entangled pairs. Our algorithm is optimal for GHZ states with 3 qubits, maximising simultaneously the final state fidelity and the rate of entanglement distribution. Furthermore, we determine the conditions yielding this simultaneous optimality for GHZ states with a higher number of qubits, and for other types of multipartite entanglement. Our algorithm is general also in the sense that it can optimise simultaneously arbitrary parameters. This work opens the way to optimally generate multipartite quantum correlations over noisy quantum networks, an important resource for distributed quantum technologies.

I. INTRODUCTION

There is a global effort put into developing a quantum internet. This quantum internet is the solution to performing distributed quantum protocols across large distances. Among these protocols we can find applications on a wide range of areas, such as quantum secure communications and computation [1–3] and quantum distributed metrology [4, 5]. Moreover, the quantum internet will have several stages of development [6] with different capabilities until a full-fledged version. Thus, a continuously evolving model of a quantum network is a solid way to describe the quantum internet, translating the physical underlying layer into a set of parameters that characterize each quantum link. While quantum communication often relies on entanglement distribution between two end-nodes, there are several possible applications that go beyond the two-party paradigm and require multipartite entanglement, which has no classical analogue. Important examples of these applications are quantum sensor networks [7–10], multi-party quantum communication [11–13] and computation [14, 15].

The current state of art in bipartite entanglement includes both protocols for entanglement generation and entanglement swapping [16], as well as tools to find the optimal way to generate entanglement between two end-nodes [17–22]. When considering multipartite entanglement, several distribution schemes, *i.e.* sequences of operations or protocols that result in the distribution of the desired state across a set of terminal nodes in a quantum network, have already been developed. In [23] a distribution scheme for GHZ and graph states is introduced, minimising the number of operations made and entangled pairs consumed, which is later used in [22] to derive bounds on achievable rates of distribution. In [24, 25] several distributions schemes are analysed and compared, also including possible intermediary purifications of entanglement. In our work are not concerned with finding the optimal scheme of distribution, but instead, un-

der a given distribution scheme, find the optimal way to distribute multipartite entanglement in a noisy quantum network. This explores a new avenue in optimal multipartite entanglement distribution, as we optimise two important parameters of the distribution. Nonetheless, our approach is easily generalizable to include more. The first parameter is the average rate for the distribution of the state. The second parameter is the fidelity of the final distributed state. We included noise by modelling each individual entangled pair using Werner states [26] and provided a description in terms of quantum channels, using its properties to calculate and verify the final state form, according to two different distributions schemes. We also consider a simpler scheme for extending bipartite entanglement inspired by the one presented in [27], without saving intermediary successes. We develop an algorithm with tools from classical routing theory [28, 29] that finds the optimal way of distributing a 3-qubit GHZ state, providing that the metrics that describe its distribution follow a set of properties. We also find the conditions that yield optimality of our algorithm when considering a higher number of qubits, under one of the possible schemes. Moreover, our methods are capable of including additional distribution parameters, while providing intuition for other possible distribution schemes.

II. QUANTUM NETWORK DESCRIPTION

Let us first describe our model of a quantum network. Structurally, it is characterised by a graph $G(V, E)$ where each node is denoted by a letter $j \in V$ and the link connecting nodes i and j is denoted by $i : j \in E$. Each path is a sequence of links and we identify them by their initial and final node $m : n$. The set of nodes $\mathcal{T} \subset V$ we want to distribute the state to is called the terminal, where $\#(\mathcal{T}) = T$ is the number of terminal nodes, or equivalently, the number of qubits of the distributed state. Each link is a noisy quantum channel,

accompanied by a classical channel, connecting neighbouring nodes which individually hold qubits in imperfect quantum memories. Each quantum channel is capable of establishing entanglement between its two nodes and each quantum node must be able to realise one and two-qubits unitary gates, as well as performing measurements on its qubits. The protocols for entanglement generation and entanglement swapping are considered to be probabilistic, following a geometrical distribution in the number of tries before the first success, similarly to what has been done in [27]. Moreover, each entangled pair of the network is modelled by a Werner state $\rho_W = \gamma |\phi^+\rangle \langle \phi^+| + (1 - \gamma)\mathbb{1}$, with $\gamma = (4F - 1)/3$, and F being the fidelity of the state. In the bipartite case, there is an equivalence between a Werner state and a representation with a depolarising channel with equal amounts of bit-flip, phase-flip and phase-bit-flip errors: $\rho_W = \mathcal{D}_1^F(|\phi^+\rangle \langle \phi^+|) = \mathcal{D}_2^F(|\phi^+\rangle \langle \phi^+|)$. This quantum channel is described in two alternate forms, one of them using the partial transposition operator Λ_i on qubit i :

$$\begin{aligned} \mathcal{D}_i^p(\rho) &= p\rho + \frac{1-p}{3}(\hat{X}_i\rho\hat{X}_i^\dagger + \hat{Y}_i\rho\hat{Y}_i^\dagger + \hat{Z}_i\rho\hat{Z}_i^\dagger) \\ &= \frac{1+2p}{3}\rho + \frac{2(1-p)}{3}\Lambda_i(\hat{Y}_i\rho\hat{Y}_i^\dagger). \end{aligned} \quad (1)$$

This equivalence is significant to find the final form of the distributed state. In addition, this trace-preserving map has important properties, among them linearity on the parameter p , commutativity for every indice i and is invariant under unitary operations applied to single qubits [30].

III. DISTRIBUTING 3-QUBIT GHZ STATES

Similarly to what has been done in [23], to distribute GHZ states we would have to first find the Steiner tree connecting the set of terminal nodes and then perform some measurements over the Steiner nodes. In this section, we will deal with the case of 3 qubits, and later we will generalise for an higher number of qubits. The reason is that, for 3 qubits, the Steiner tree connecting 3 terminal nodes is always a star-graph, and the scheme is equivalent to first distributing bipartite entanglement between every terminal and a center node and then performing a set of operations on the center node. Thus, the central idea is finding the center node for which this results in the optimal solution. To define optimal, we must concern the metrics for the distribution of this entangled state, namely the rate of distribution and the final state fidelity.

Consider that the center node, c , is capable of coordinating every process. There is an initial phase to signal the beginning of bipartite entanglement distribution, followed by the phase of creating bipartite entanglement in every branch connecting to the center node and finally performing the set of operations that result in the desired state distribution. Following [17], we can provide a

measure for the average rate of distribution, ξ , considering the different steps in this scheme. This average rate is given by the inverse of the average time, T , it takes to complete the distribution. Considering a scheme of attempts until the first success, if any branch fails to create bipartite entanglement, every branch starts over, the final distribution of the probability of the first success will follow a geometric distribution. In such case, the average time it would take to completely distribute the multipartite entangled state would be the communications time multiplied by the average number of attempts before the first success:

$$T_{tree} = 2 \cdot \frac{\max_{\tau \in \mathcal{J}} \{t_{c:\tau}\}}{\prod_{\tau \in \mathcal{J}} p_{c:\tau}}, \quad \xi_{tree} = \frac{1}{T_{tree}} \quad (2)$$

where $p_{c:\tau}$ and $t_{c:\tau}$ correspond, respectively, to the probability of success and communications time of the path $c : \tau$. If the operations performed in each Steiner node are not deterministic, this time will increase by multiplying the expected value of the stochastic process that characterizes the global set of operations. As for the fidelity and form of the distributed state, it is equivalent to applying a depolarising channel to each terminal node substituting the p value in Eq. 1 by the fidelity $F_{c:\tau} \equiv F_\tau$ correspondent to each branch connecting the center node c to the terminal τ . The final fidelity of this state can be obtained, with the second description of the depolarising channel revealing to be particularly useful. The result is:

$$f = \frac{1}{2} \left[\prod_{\tau \in \mathcal{J}} \frac{1+2F_\tau}{3} + \prod_{\tau \in \mathcal{J}} \frac{2(1-F_\tau)}{3} + \prod_{\tau \in \mathcal{J}} \frac{4F_\tau - 1}{3} \right] \quad (3)$$

Using Eqs. 2-3, a map between the T paths parameters and the tree rate of distribution and fidelity of the final state is therefore obtained:

$$\left\{ [p_{c:\tau}, t_{c:\tau}, F_{c:\tau}] \right\}_{\tau \in \mathcal{J}} \mapsto [\xi_{tree}, f_{tree}] \quad (4)$$

In each branch connecting nodes m to n , we must consider a distribution of bipartite entanglement depending on four parameters, among them the probability of success of distributing end-to-end entanglement $p_{m:n}$, the classical communications time $t_{m:n}$, the fidelity expressed in γ values $\gamma_{m:n}$ and the memory decoherence time $\sigma_{m:n}$ (detailed description is provided in Appendix A). These four parameters are then contracted to three:

$$[p_{m:n}, t_{m:n}, \gamma_{m:n}, \sigma_{m:n}] \mapsto [p_{m:n}, t_{m:n}, F_{m:n}], \quad (5)$$

subject to $(4F_{m:n} - 1)/3 = \gamma_{m:n} e^{-t_{m:n}/\sigma_{m:n}}$. Later, it becomes the input for Eq. 4, under a proper choice of nodes m and n (see Fig.1). Nonetheless, the four parameters which are the input of Eq. 5 must be routed separately for the optimal paths to be found and consequently, the optimal star, under appropriate algorithms.

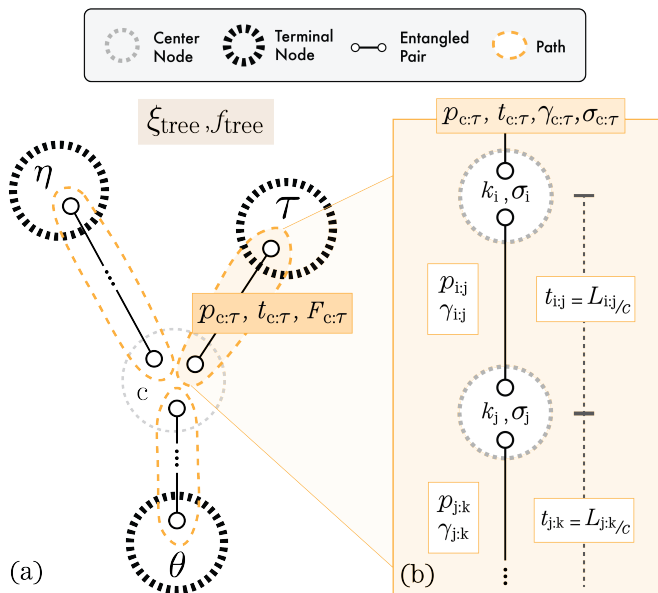


FIG. 1. (a) Star composed by 3 different paths, connecting terminal nodes τ , η and θ to the center node c . Notice that the rate ξ_{tree} depends on each branch probability of success $p_{c:\tau}$ and communications time $t_{c:\tau}$ (Eq. 2). Moreover, the fidelity of the final state f_{tree} depends on each branch fidelity $F_{c:\tau}$ (Eq. 3). (b) Branch composed by an arbitrary number of links. Each branch final fidelity $F_{c:\tau}$ depends on the path γ values $\gamma_{c:\tau}$, communications time $t_{c:\tau}$ and memory decoherence time $\sigma_{c:\tau}$. The other parameters, namely the probability of success $p_{c:\tau}$ and communications time $t_{c:\tau}$ are independent.

IV. ALGORITHMS FOR OPTIMAL MULTIPARTITE ENTANGLEMENT DISTRIBUTION

Now that we can characterize both the rate of distribution and fidelity of the final state, we need to find the optimal star. Here, the definition of optimal is crucial. In the case we only deal with one parameter, *e.g.* the fidelity, there only exists one optimal solution, unless several solutions have the same fidelity. However, if we want to consider more parameters to optimise, a multi-objective approach is necessary. In [31], multi-objective shortest-paths (MOSP) algorithms are introduced by defining the dominance relation and using the Pareto optimality definition. This comes from the fact that, when dealing with multi-objective routing while one path might be better for some parameters, another path might be better for other parameters. This results in a set of optimal solutions that is usually larger than one - the Pareto front. The same relation is also valid and central for finding the optimal way to distribute a 3-qubit GHZ state. From the scheme for creating a 3-qubit GHZ state definition, the main problem is finding the correct center node such that the corresponding star is optimal, depicted in *Algorithm 1*. In [28, 32], a more fundamental definition for these metrics involved in routing problems is introduced using algebras for routing. We will use both terms, metrics

and algebras, to refer to the same thing. They contain a structured algebraic definition of the metric using sets to describe the space of the parameters, binary operations to define how paths are extended and total-orders to define the ordering of the parameters, *i.e.* which one is the better:

Definition 1. Algebra for Routing is an ordered septet $(W, \preceq, L, \Sigma, \phi, \oplus, f)$ comprised as follows: W a set of weights, \preceq a total order, L a set of labels, Σ a set of signatures, ϕ a special signature, \oplus a binary operation that maps pairs of labels and signatures into a signature and a function f that maps signatures into weights.

Using this definition of algebras for routing [28], some properties can be defined which guarantee the optimality under an appropriate algorithm, namely monotonicity and isotonicity:

Definition 2. (Monotonicity) an algebra for routing is called monotone if: $\forall l \in L; \alpha \in \Sigma : f(\alpha) \preceq f(\alpha \oplus l)$.

Definition 3. (Isotonicity) an algebra for routing is called isotone if: $\forall l \in L; \alpha, \beta \in \Sigma : f(\alpha) \preceq f(\beta) \Rightarrow f(\alpha \oplus l) \preceq f(\beta \oplus l)$.

The same reasoning can be made for trees, creating algebras for trees. Here, the labels define paths, instead of edges, and signatures define trees, instead of paths. Using these algebras for trees, another property arises, enabling that the shortest-tree necessarily contains the possible shortest-paths if the schemes for creating paths and trees are different. This property is what we called label-isotonicity:

Definition 4. (Label-isotonicity) An algebra for trees $(W, \preceq, \Sigma, \Xi, \phi, \oplus, f)$ is said to be label-isotone if [33]: $\forall \sigma_1, \sigma_2 \in \Sigma; t \in \Xi : \sigma_1 \preceq \sigma_2 \Rightarrow f(t \oplus \sigma_1) \preceq f(t \oplus \sigma_2)$

Algorithm 1 Algorithm for T-Star

```

1: procedure T-STAR EXACT(terminal)
2:    $A :=$  Set of solutions initialised empty;
3:   for  $node \in terminal$  do
4:     procedure SHORTEST-PATH(node);
5:    $Nodes_{reach} \leftarrow$  Nodes reachable from every terminal;
6:   for  $node \in Nodes_{reach}$  do
7:     for Tree  $T = \cup_{i,j} Path^j(node, terminal_i)$  do
8:       if  $T$  is non-dominated by every tree in  $A$  then
9:         Add  $T$  to  $A$ ;

```

Proposition 1. For the shortest-star with 3 terminals, the paths connecting the center node and the terminals must be the shortest-paths, if the underlying algebras for trees are label-isotone.

Proposition 1 (proof detailed in Appendix B) provides that *Algorithm 1* converges to the set of optimal solutions for the 3-qubit GHZ state problem, given that the paths are optimal in the Pareto sense and that the underlying algebras for trees are monotone and label-isotone.

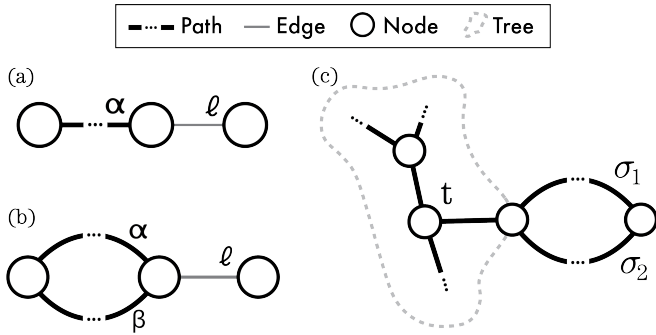


FIG. 2. Illustration of the context in the algebras' properties. (a) Monotonicity. (b) Isotonicity. (c) Label-isotonicity.

Moreover, further refinements in the search process can be obtained, taking advantage of properties of the algebras. Namely, if the algebra for trees is monotone, then a necessary, but not sufficient, condition for existence of a shortest-tree connecting the set of terminal can be obtained: if there is no possible path connecting some pair of terminals, then there is no solution of the problem. From the structure of the algorithm, this condition can be implemented while finding the shortest-paths from each terminal node. Providing that the solution for the MOSP algorithms are optimal, further detailed in Appendix C, it can also be verified that both the rate of distribution and fidelity of the final state are monotone and label-isotone for any number of qubits in the star scheme (see Appendices E and F), therefore ensuring optimality of *Algorithm 1*.

V. DISTRIBUTING N-QUBIT GHZ STATES

When considering a higher number of qubits, there are two possible schemes to distribute this state. The first scheme - star scheme - is an extension of 3-qubits resembling a star-graph, hence its name. Identically, it consists of generating bipartite entanglement between every terminal node and a center node, which can ultimately be any of the terminal nodes, and then projecting every qubit of the center node in the desired state. This scheme is capable of distributing any multipartite entangled state, besides GHZ states. Using *Algorithm 1* for this scheme also leads to optimality under the same constraints on the algebras, if the same link can be used more than once. If the latter is not true and this condition is only imposed *a posteriori*, then we can only extract at least a part of the set of optimal solutions and flag if there might exist other optimal solutions or not. For 3 qubits, this condition did not matter since, if there is an overlap of links used, then there is always another star that is better, with the center node in another position.

The other possible scheme is the tree scheme [23], detailed in Appendix D, which is always either equal or better at distributing GHZ states. It is more efficient

in the bigger number of terminals limit, since it almost surely reduces the number of entangled pairs consumed. However, it can not be used to distribute some states, such as a W state. Nonetheless, for only 3 qubits, both schemes are identical, differing only up to local operations.

VI. SIMULATIONS

In *Figure 3* we present the scaling of the complexity of this algorithm in two different types of networks, namely Erdős-Rényi networks [34, 35], with an approximate scaling of individual link fidelities that guarantee the network remains connected [37], and random geometric networks [38], which convey the limitation in the length of each individual link in a quantum network [39]. Every link has a

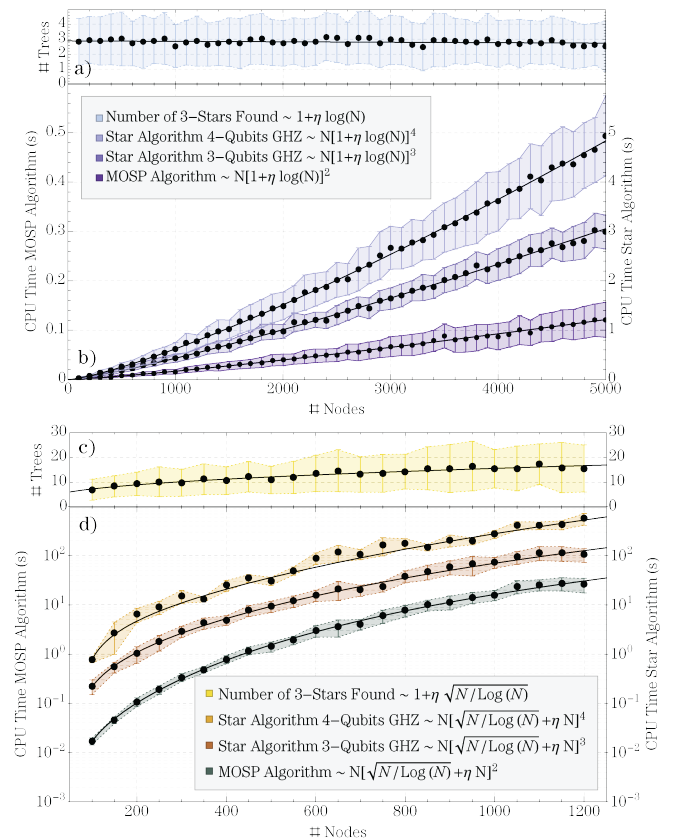


FIG. 3. Simulations for MOSP algorithm and *Algorithm 1* for 3 and 4 qubits GHZ state distribution in (b) Erdős-Rényi networks with average degree $\langle \lambda \rangle = 3$ and (d) random geometric networks with average degree $\langle \lambda \rangle = 8$, displaying as well the average number of solutions found for *Algorithm 1* applied to the 3-qubits problem in (a) Erdős-Rényi networks and (c) random geometric networks. The parameters utilised were the following: $p_{\min} = 0.5$, $t_{\min} = 1$, $t_{\max} = 100$, $\sigma_{\min} = 10^4$, $\sigma_{\max} = 10^5$, $f_{\text{trunc}}^{\text{GHZ}} = 0.5$, $f_{\text{trunc}}^{\text{path}} = 0.9$. For a Erdős-Rényi network $\alpha = 2$ and $d_{\max} = \log N / \log \langle \lambda \rangle$ [34, 35]. For random geometric networks $\alpha = 2$ and $d_{\max} = \sqrt{N / \log N}$ [36].

value of fidelity uniformly distributed in $[f_{\min}, 1)$, a probability of successful entanglement generation and probability of successful entanglement swapping distributed uniformly in $[p_{\min}, 1)$. The communications time and memory decoherence times are distributed in $[t_{\min}, t_{\max}]$ and $[\sigma_{\min}, \sigma_{\max}]$, respectively. The values of f_{\min} scale approximately through a power law $f_{\min} \sim [f_{\text{trunc}}]^{\alpha/d_{\max}}$ [37] that guarantee each path contains entanglement and the final distributed state fidelity $f_{\text{trunc}}^{\text{GHZ}} > 1/2$. Notice that f_{trunc} is usually $1/2$, value for which entanglement is known to be present. However, in our case, to guarantee that most of the simulations would result in finding optimal stars with $f_{\text{trunc}}^{\text{GHZ}} > 1/2$, we set the value of each path $f_{\text{trunc}}^{\text{path}} = 0.9$.

VII. CONCLUSIONS

We have calculated the effect of imperfect entanglement in the distribution of multipartite entanglement, namely GHZ states, over noisy quantum networks. Our methods are capable of being extended to other quantum states. We used tools from classical routing theory to describe quantum networks and the parameters to optimise. This was crucial to define a metric for both the fidelity and rate of distribution, realising an algorithm capable of distributing these states under the star scheme in the optimal way, while providing the necessary conditions to attain this optimality. Moreover, our approach is compatible with previously known algorithms that take advantage of metric properties to optimize algorithm runtimes, including both methods for single-objective or multi-objective optimisation.

By separating our approach into two equivalent layers, described by distinct algebras for routing and for trees, we allow bipartite entanglement distribution to be different from multipartite schemes. This creates the space for different protocols or algorithms within each layer. As one can see, while finding the optimal paths, we had to separate different parameters that played along in the end, namely the fidelity, depending on the quantum memories and communications time. This was done to ensure the optimality of our algorithm, since considering

them together when routing resulted in a non-isotonic algebra. This is an example of how our approach can accommodate other parameters of distribution. While some metric depending on several parameters might not have the required properties, there might exist a decomposition into other metrics that verify them. Of course, by increasing the number of objectives of optimization, the algorithms runtime also increases. This is in part derived from the fact that the set of optimal solutions grows. Moreover, we establish that when considering GHZ states with an number of qubits more than 3, then this optimality is guaranteed for the star-scheme distribution if we allow if link to be used more than once. Nonetheless, using these classical techniques and tools, we can prove the conditions that yield the optimality of our work as well as creating the necessary formulation to expand the methodology.

Furthermore one could apply this same methodology to different distribution schemes [40], introducing entanglement purification rounds in the bipartite distribution scheme [25] or even different quantum repeater protocols [41], opening the way to optimally generate multipartite entanglement over noisy quantum networks. This is important to understand how the quantum internet must evolve so distributed quantum technologies, namely distributed quantum sensing becomes capable of going beyond the classical bounds of precision and realising the quantum advantage that can be attained using multipartite entanglement [42, 43].

ACKNOWLEDGMENTS

The authors thank D. Markham for useful comments on the work. Furthermore, the authors thank the support from Fundação para a Ciência e a Tecnologia (Portugal), namely through project UIDB/50008/2020 and QuantSat-PT, as well as from projects TheBlinQC and QuantHEP supported by the EU H2020 QuantERA ERA-NET Cofund in Quantum Technologies and by FCT (QuantERA/0001/2017 and QuantERA/0001/2019, respectively), and from the EU H2020 Quantum Flagship projects QIA (820445) and QMiCS (820505).

-
- [1] C. H. Bennett and G. Brassard, *Theoretical Computer Science* **560**, 7 (2014).
 - [2] A. I. Nurhadi and N. R. Syambas, *Proceeding of 2018 4th International Conference on Wireless and Telematics, ICWT 2018*, 18 (2018).
 - [3] A. Broadbent, J. Fitzsimons, and E. Kashefi, *Proceedings - Annual IEEE Symposium on Foundations of Computer Science, FOCS*, 517 (2009), arXiv:0807.4154.
 - [4] I. L. Chuang, *Phys. Rev. Lett.* **85**, 2006 (2000).
 - [5] D. Gottesman, T. Jennewein, and S. Croke, *Phys. Rev. Lett.* **109**, 070503 (2012).
 - [6] S. Wehner, D. Elkouss, and R. Hanson, *Science* **362**, 6412 (2018).
 - [7] C. Ren and H. F. Hofmann, *Phys. Rev. A* **86**, 014301 (2012).
 - [8] E. T. Khabiboulline, J. Borregaard, K. De Greve, and M. D. Lukin, *Phys. Rev. A* **100**, 022316 (2019).
 - [9] Z. Eldredge, M. Foss-Feig, J. A. Gross, S. L. Rolston, and A. V. Gorshkov, *Phys. Rev. A* **97**, 042337 (2018).
 - [10] T. Qian, J. Bringewatt, I. Boettcher, P. Bienias, and A. V. Gorshkov, (2020), arXiv:2011.01259.
 - [11] M. Hillery, V. Bužek, and A. Berthiaume, *Phys. Rev. A*

59, 1829 (1999).

[12] C. Zhu, F. Xu, and C. Pei, *Sci. Rep.* **5**, 17449 (2015).

[13] G. Murta, F. Grasselli, H. Kampermann, and D. Bruß, *Adv. Quantum Technol.* **3**, no. 11, p. 2000025 (2020).

[14] E. D'Hondt and P. Panangaden, *Quantum Inf. Comput.* **6**, 173 (2004).

[15] R. Raussendorf and H. J. Briegel, *Phys. Rev. Lett.* **86**, 5188 (2001).

[16] W. Munro, K. Azuma, K. Tamaki, and K. Nemoto, *IEEE J. Sel. Top. Quantum Electron.* **21**, no. 3, p. 78-90 (2015).

[17] M. Caleffi, *IEEE Access* **5**, 22299 (2017).

[18] K. Chakraborty, F. Rozpedek, A. Dahlberg, and S. Wehner, (2019), arXiv:1907.11630.

[19] S. Shi and C. Qian, (2019), arXiv:1909.09329.

[20] C. Li, T. Li, Y.-X. Liu, and P. Cappellaro, *npj Quantum Inf.* **7**, 10 (2021).

[21] W. Dai, T. Peng, and M. Z. Win, *IEEE Journal on Selected Areas in Communications* **38**, 540 (2020).

[22] S. Bäuml, K. Azuma, G. Kato, and D. Elkouss, *Commun. Phys.* **3**, 55 (2020).

[23] C. Meignant, D. Markham, and F. Grosshans, *Phys. Rev. A* **100**, 052333 (2019).

[24] J. Wallnöfer, A. Pirker, M. Zwerger, and W. Dür, *Sci. Rep.* **9**, 314 (2019).

[25] K. Goodenough, D. Elkouss, and S. Wehner, *Phys. Rev. A* **103**, 032610 (2021).

[26] R. F. Werner, *Phys. Rev. A* **40**, 4277 (1989).

[27] S. Brand, T. Coopmans, and D. Elkouss, *IEEE J. Sel. Areas Commun.* **38**, 619 (2020).

[28] J. L. Sobrinho, *IEEE/ACM Trans. Netw.* **13**, 1160 (2005).

[29] S. Demeyer, J. Goedgebeur, P. Audenaert, M. Pickavet, and P. Demeester, *4or* **11**, 323 (2013).

[30] M. Hein, W. Dür, J. Eisert, R. Raussendorf, M. Van Den Nest, and H. J. Briegel, *Proceedings of the International School of Physics "Enrico Fermi"*, **162**, 115 (2006).

[31] E. Q. V. Martins, *Eur. J. Oper. Res.* **16**, 236 (1984).

[32] J. L. Sobrinho, in *Comput. Commun. Rev.* **33**, 49-60 (2003).

[33] By $\sigma_1 \preceq \sigma_2$ we mean $f(\sigma_1 \oplus e_\Sigma) \preceq f(\sigma_2 \oplus e_\Sigma)$ where e_Σ is the neutral element of Σ w.r.t \oplus .

[34] A.-L. Barabási and M. Pósfai, *Network science* (Cambridge University Press, Cambridge, 2016).

[35] S. N. Dorogovtsev, A. V. Goltsev, and J. F. F. Mendes, *Rev. Mod. Phys.* **80**, 1275 (2008).

[36] R. B. Ellis, J. L. Martin, and C. Yan, *Algorithmica* **47**, 421 (2007).

[37] B. C. Coutinho, W. J. Munro, K. Nemoto, and Y. Omar, (2021) arXiv:2103.03266.

[38] J. Dall and M. Christensen, *Phys. Rev. E* **66**, 016121 (2002).

[39] T. Inagaki, N. Matsuda, O. Tadanaga, M. Asobe, and H. Takesue, *Optics Express* **21**, 23241 (2013).

[40] J. Wallnöfer, M. Zwerger, C. Muschik, N. Sangouard, and W. Dür, *Phys. Rev. A* **94**, 052307 (2016).

[41] T. Satoh, K. Ishizaki, S. Nagayama, and R. Van Meter, *Phys. Rev. A* **93**, 032302 (2016).

[42] P. Sekatski, S. Wölk, and W. Dür, *Phys. Rev. Research* **2**, 023052 (2020).

[43] N. Shettell, W. J. Munro, D. Markham, and K. Nemoto, (2021), arXiv:2101.02823.

[44] Y. neng Guo, Q. long Tian, K. Zeng, and Z. da Li, *Quantum Inf. Process.* **16**, 12 (2017).

[45] X. Wang, *Exact algorithms for the Steiner Tree Problem*,

(2008).

[46] G. Robins and A. Zelikovsky, *SIAM J. Discrete Math.* **19**, 1 (2005).

Appendix A: Bipartite Entanglement Distribution

In this section, we detail the used metrics for bipartite entanglement distribution across a chain of quantum links, or path. We do this in a way that guarantees each metric is both monotonic and isotonic, so to ensure that a general MOSP algorithm converges to the optimal solution.

Starting with the probability of success, denote by $p_{i:j}$ the probability of successful entanglement generation between neighbouring nodes i and j at the first attempt and by k_j the probability of successful entanglement swapping on node j also at the first attempt. Since every stochastic process is independent, the probability of success of generating end-to-end entanglement across a chain of quantum nodes will also be geometrically distributed with a probability of success at the first attempt given by:

$$p_{m:n} = \prod_{i:j \in m:n} p_{i:j} \prod_{j \in m:n \setminus m,n} k_j. \quad (\text{A1})$$

The classical communications time will also play an important role in the rate and each branch fidelity. We denote by $t_{i:j} = L_{i:j}/c$ the time it takes to send a classical message between neighbouring nodes i and j , distanced by $L_{i:j}$. In our simplified model, there are two rounds of classical communication across the chain: one for communicating successful entanglement generation across every link of the chain and another to communicate successful entanglement swapping in every node of the chain, with correspondent corrections. This takes two times the sum of each individual time across the chain to complete each successful round:

$$t_{m:n} = 2 \sum_{i:j \in m:n} t_{i:j}. \quad (\text{A2})$$

As for the fidelity across a chain after the entanglement swapping was completed, taking advantage of the γ change of variables described in the main text $\gamma = (4F - 1)/3$, results in a simple multiplication of each γ value along the chain. Using γ we have a threshold value at $1/3$, meaning that below this threshold, entanglement does no longer exist and the path can not be used:

$$\gamma_{m:n} = \begin{cases} \prod_{i:j \in m:n} \gamma_{i:j}, & \gamma_{m:n} \geq 1/3 \\ 0, & \gamma_{m:n} < 1/3. \end{cases} \quad (\text{A3})$$

In order to include the quantum memory decoherence time, similarly to what has been done in [27, 44], we adapted the contributions to our simpler scheme. Consider that, for Bell states, the effect of memory decoherence in the fidelity of the state verifies $\gamma \mapsto \gamma \cdot e^{-t_{wait}/\sigma}$,

where σ is the quantum memory decoherence time. In the first round, if the generation is successful, entanglement is stored between every neighbouring node of the chain. Therefore, the memory decoherence factor of each node except the first and the last contribute two times for the final state distribution. On the second round, if the swapping is successful, the entanglement is held only within the first and the last node. This results in every node contributing the same to the decoherence factor, given that the communications time is identical:

$$\frac{1}{\sigma_{m:n}} = \sum_{i \in m:n} \frac{2}{\sigma_i}. \quad (\text{A4})$$

By routing these four parameters independently, we can guarantee that the contraction from these four parameters into only three parameters detailed in the main text provides the optimal solutions.

Appendix B: Dominance Relation and Proposition 1 Proof

Before stepping onto the proof for *Proposition 1*, let us first dive into the dominance relation, so to generalise this result for any set of objectives. Given a set of algebras for routing $\{(W^i, \preceq^i, L^i, \Sigma^i, \phi^i, \oplus^i, f^i)\}$, as introduced in [31], the dominance relation is given by the following definition:

Definition 5. (*Dominance*) let ω and ν be two different signatures in $\{\Sigma^i\}$. ω dominates ν , $\omega D \nu$ if $f^j(\omega^j) \preceq^j f^j(\nu^j) \forall j \in \{1, \dots, k\}$ and the strict order holds at least once.

We will first present the proof for the case of one objective of routing, or only one algebra, using only its total order and then generalise for the case of an arbitrary number of objectives using the dominance relation. Moreover, we will do this for a star with an arbitrary number of terminals.

Proof. Proposition 1 - Consider the more general case that the center node is connected by n paths (this does not happen if the center node is one of the terminals, but for that case consider the star composed of $n - 1$ paths), indexed by a number between 1 and n : $path_1, path_2, \dots, path_n \in \Sigma$. Each path is connected to one of the n terminals. Fix all paths but $path_1$. Let $t \in \Xi$ be correspondent to the tree formed by $path_2 \cup path_3 \cup \dots \cup path_n$. Now consider there $\exists \overline{path_1} : \overline{path_1} \preceq path_1$, due to label-isotonicity of the algebra for trees, then if $\overline{path_1} \preceq path_1 \Rightarrow f(t \oplus \overline{path_1}) \preceq f(t \oplus path_1)$ and the shortest tree would be $\overline{path_1} \cup path_2 \cup path_3 \cup \dots \cup path_n$. Doing this for every other path, we get that the shortest-star is the one with every branch being the shortest-path between the center node and the terminals. \square

Remark. *The same applies for the multi-objective shortest-star problem, with the paths being the set of*

Pareto-Optimal paths and requiring that every algebra for trees is label-isotone.

Proof. Consider that $path_1 \notin X_1$ where X_1 is the set of Pareto-Optimal paths between the node 1 and the center node. Then, $\exists \overline{path_1} \in X_1$ such that $\overline{path_1} D path_1$ and from here the star containing $\overline{path_1}$ is better than the one containing $path_1$. This comes from the how the dominance relation is defined. The rest of the proof is identical to the previous proof. \square

One important consideration is that the algebras for trees and the algebras for routing (parameters for trees and parameters for paths) do not need to be equal in number nor in form. As long as each algebra for routing is individually monotone and isotone, then the set of paths are optimal under an appropriate algorithm, which we will exemplify in *Appendix C*. And if each algebra for trees is label-isotone with respect to each individual algebra for routing it depends on, then this optimality is guaranteed.

Notice that in this proof we do not concern with different paths having intersections, as for the case with only three terminals, $T = 3$, this is never the case. For $T > 3$ our approach is only optimal if we allow intersection, which are equivalent to letting the same link be used more than once. If that is not the case, we can only extract at least part of the solutions and flag if there might exist more or not. If after running the algorithm and finding all possible solutions, and none of them have intersections, then all the optimal solutions were found. However, if some have intersections, then we can discard them (this is what we mean when we say *a posteriori*) but we can not guarantee all optimal solutions were found, since we ignored some solutions with non-optimal paths that did not have intersections. This can be translated in the following way: consider there exists a star $s = s_1 \oplus p_1$ such that $s_1 \cap p_1 \neq \emptyset$, this is, they share a common link, and that $s \in SA \equiv$ algorithm solutions. Now, consider there $\exists \tilde{p}_1 : p_1 D \tilde{p}_1$ and $\tilde{s} = s_1 \oplus \tilde{p}_1$ and $s_1 \cap \tilde{p}_1 = \emptyset$, there is a chance of \tilde{s} being in SA . If however, every solution in SA has no intersections and the algorithm is optimal, it would mean that any star with a non-optimal path, intersecting or not, would be dominated by at least one of the solutions and therefore would not be optimal.

Appendix C: MOSP Algorithm

The multi-objective shortest-path (MOSP) algorithm is a powerful tool to find the optimal path in the Pareto sense, which is then the input for our algorithm of distributing multipartite entanglement. We implemented it in the following way, finding every optimal path from the source to every other node of the network:

Algorithm 2 Multi-Objective Routing

```

1: procedure SHORTEST-PATH(source)  $\triangleright$  Finds the
   shortest path to every node from the source
2:   Nodes := Set of nodes of the network, each with un-
   derlying list of paths  $Paths_u$  initialised as empty;
3:   A := Set of visited nodes of the network initialised as
   empty;
4:   B := Set of nodes to visit ordered as a priority queue
   data structure, with priority defined by the dominance
   relation;
5:   Initialise  $source \leftarrow \{e_{\Sigma_i}\}$ ;
6:   Add source to B;
7:   while B  $\neq$  empty do
8:     node  $\leftarrow$  Top(B)
9:     Remove node from B and add to A;
10:    for  $v \in$  neighbours(node) do
11:       $Paths^{add} \leftarrow$  possible paths from  $\{Paths_{node}^{(i)} \oplus$ 
   Edge(node, v) $\}$ ;
12:      if  $Paths_v =$  empty then
13:         $Paths_v \leftarrow Paths^{add}$ ;
14:        Add v to B;
15:      if  $Paths_v \neq$  empty then
16:         $Paths^p \leftarrow$  non-dominated paths of
    $Paths^{add} \cup Paths_v$ ;
17:        if  $Paths^p \neq Paths_v$  then
18:           $Paths_v \leftarrow Paths^p$ 
19:          if  $v \in A$  then
20:            Add v to B and remove from A;
21:          if  $v \notin A$  then
22:            Update v in B;

```

where $\{e_{\Sigma_i}\}$ are the neutral elements of Σ_i w.r.t \oplus_i . The main reason we had to separate the fidelity metric

$$\frac{4F_{m:n} - 1}{3} = \gamma_{m:n} e^{-t_{m:n}/\sigma_{m:n}} \quad (C1)$$

into three different metrics is that, while this parameters are individually monotonic and isotonic, together they are not. Then using this type of algorithm would fail at converging to the optimal solution that maximises $F_{m:n}$. However, by separating them and treating them independently using the dominance relation, one can clearly see that, if one path dominates the other then:

$$\left\{ \begin{array}{l} \gamma_{m:n}^{(1)} \geq \gamma_{m:n}^{(2)} \\ t_{m:n}^{(1)} \leq t_{m:n}^{(2)} \\ \sigma_{m:n}^{(1)} \geq \sigma_{m:n}^{(2)} \end{array} \right\} \implies F_{m:n}^{(1)} \geq F_{m:n}^{(2)}$$

If the left hand side is not true, then the paths do not dominate each other and we can not guarantee that at every extension, the relation of the final fidelities would maintain, requiring us to keep track of all the non-dominated paths - which constitute the set of Pareto optimal paths.

Appendix D: Tree-Scheme

The tree scheme [23] consists of a generalisation of the star scheme, when we allow the topology of distri-

bution to be any tree, not just a star-graph. Starting from a tree-graph connecting all terminal nodes (see *Figure 4b*), choosing a leaf node and iteratively applying the star expansion protocol [23] for every node will result in GHZ state distributed across the terminal nodes. Under this distribution scheme, finding the optimal way to distribute entanglement across the network is equivalent to finding the shortest-tree connecting the terminal nodes, under a given set of parameters. This is translatable to solving the multi-objective Steiner tree algorithm with the corresponding metrics. The regular Steiner tree problem is known to be *NP-Hard* [45, 46] and adding the multi-objective setup quickly escalates the problem complexity. On the other hand, finding the shortest-star connecting a set of terminal nodes is a more tractable problem, and a reason why for 3-qubits, this problem is feasible.

To find the metrics expression for the n -qubits GHZ state distributed in a tree-scheme, we considered one center of coordination in order to minimise the communications time. This center of coordination, in the case of the star scheme was trivially the center node. Now, since the coordinating node is not necessarily one branch away from every terminal node, we have to perform a minimisation over the possible locations for this node:

$$T_{tree} = 2 \cdot \frac{\min_{s \in \mathcal{S}} \left\{ \max_{\tau \in \mathcal{T}} \{t_{s:\tau}\} \right\}}{\prod_{m:n \in \text{branches}} p_{m:n}}, \quad \xi_{tree} = 1/T_{tree} \quad (D1)$$

Where \mathcal{S} is the set of the Steiner nodes, *i.e* the set of nodes that belong to the tree, but are not terminal nodes. In our case, they are always intersections of branches.

Moving to the fidelity and form of the distributed state: we must start from one terminal node, τ_0 , making the result dependent from which terminal we apply the procedure. This does not invalidate the scheme described when calculating the rate, since this only affects which

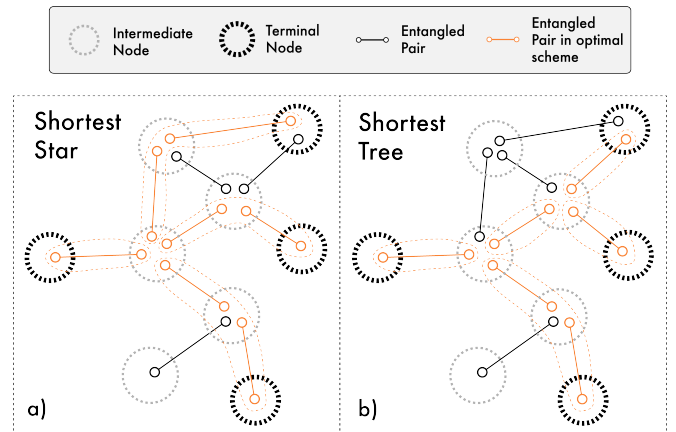


FIG. 4. In these figures we provide an example of what a shortest tree and a shortest star are, highlighted in orange. Keep in mind that groups, or paths, surrounded by a traced orange line are equivalent to an entangled pair after bipartite entanglement distribution.

operations are made. Starting from an initial node, after performing the star-expansion protocol across all of the intermediary nodes of the tree, the final form of the GHZ state is equivalent, up to SWAP operations which leave in GHZ portion invariant and the fidelity unaffected, to applying a depolarising channel to each terminal node except the initial and applying, for each Steiner node, a depolarising channel to the initial node. The fidelities of each depolarising channel correspond to the fidelities of each branch connecting either the terminals or Steiner nodes, respectively. The final fidelity of this state can be calculated, with the second description of the depolarising channel revealing again to be particularly useful. The result is:

$$f = \frac{1}{2} \left[E(\mathcal{S}) \prod_{\tau \in \mathcal{J} \setminus \tau_0} \frac{1 + 2F_\tau}{3} + O(\mathcal{S}) \prod_{\tau \in \mathcal{J} \setminus \tau_0} \frac{2(1 - F_\tau)}{3} + \prod_{s \in \mathcal{S}} \frac{4F_s - 1}{3} \cdot \prod_{\tau \in \mathcal{J} \setminus \tau_0} \frac{4F_\tau - 1}{3} \right] \quad (\text{D2})$$

Where the functions $E(\mathcal{S})$ and $O(\mathcal{S}) = 1 - E(\mathcal{S})$ correspond to the even and odd applications of $2(1 - F_i)/3 \cdot \Lambda_i(\hat{Y}_i \rho \hat{Y}_i^\dagger)$, respectively. Moreover, since every star is a tree, these metrics also apply for the star-scheme under the correct assumptions. It is easy to verify that in a star scheme, there is only one Steiner node which translates in the functions $E(\mathcal{S})$ and $O(\mathcal{S})$ taking the values $(1 + 2F_{\tau_0})/3$ and $2(1 - F_{\tau_0})/3$ respectively.

Appendix E: Monotonicity

In this section we will prove that every algebra for trees used is monotone, for both the star-scheme and the tree scheme detailed previously. Starting with the fidelity for the more general GHZ state, under any of the possible schemes which are detailed in the main text, we have to prove that the addition of any path to the tree results always in a worse fidelity.

For this, let us first understand a little better the functions $E(\mathcal{S})$ and $O(\mathcal{S}) = 1 - E(\mathcal{S})$, which as told, correspond to the even and odd applications of $2(1 - F_i)/3 \cdot \Lambda_i(\hat{Y}_i \rho \hat{Y}_i^\dagger)$, respectively. Beware of the following properties of these functions:

$$\begin{cases} E(\mathcal{S}) \geq O(\mathcal{S}) \\ E(\mathcal{S} \oplus s) = E(\mathcal{S}) \cdot F_s + O(\mathcal{S}) \cdot \bar{F}_s \\ O(\mathcal{S} \oplus s) = O(\mathcal{S}) \cdot F_s + E(\mathcal{S}) \cdot \bar{F}_s \\ E(\mathcal{S}) - E(\mathcal{S} \oplus s) = [E(\mathcal{S}) - O(\mathcal{S})] \cdot \bar{F}_s \\ O(\mathcal{S} \oplus s) - O(\mathcal{S}) = [E(\mathcal{S}) - O(\mathcal{S})] \cdot \bar{F}_s \end{cases} \quad (\text{E1})$$

For simplicity, take only in this section, $F_s \equiv (1 + 2F_s)/3$ and $\bar{F}_s = 1 - F_s$. Consider one tree is described by the following signature

$$\{E(\mathcal{S}) \cdot a, O(\mathcal{S}) \cdot b, c\}.$$

After performing an extension with another path, there are two possible options. Either the path connects to a terminal node τ or to a Steiner node s . In the case it connects to a terminal node, the metric is trivially monotonic since every element in the signature would be multiplied by a value smaller than one:

$$\begin{Bmatrix} E(\mathcal{S}) \cdot a \\ O(\mathcal{S}) \cdot b \\ c \end{Bmatrix} \mapsto \begin{Bmatrix} E(\mathcal{S}) \cdot a \cdot F_\tau \\ O(\mathcal{S}) \cdot b \cdot \bar{F}_\tau \\ c \cdot (F_\tau - \bar{F}_\tau) \end{Bmatrix}$$

In the case the path connects to a Steiner node then we would have to prove that:

$$\begin{aligned} & \begin{cases} E(\mathcal{S} \oplus s) \cdot a + O(\mathcal{S} \oplus s) \cdot b \leq E(\mathcal{S}) \cdot a + O(\mathcal{S}) \cdot b \\ c \cdot (F_s - \bar{F}_s) \leq c \end{cases} \\ \Leftrightarrow & \begin{cases} [O(\mathcal{S} \oplus s) - O(\mathcal{S})] \cdot b \leq [E(\mathcal{S}) - E(\mathcal{S} \oplus s)] \cdot a \\ c \cdot (F_s - \bar{F}_s) \leq c \cdot 1 = c \end{cases} \\ \Leftrightarrow & \begin{cases} b \leq a \\ - \end{cases} \end{aligned} \quad (\text{E2})$$

Which is always true since $0 \leq b \leq (1/3)^n < (2/3)^n \leq a \leq 1$ and $F_s - \bar{F}_s \leq 1$. This proves the monotonicity of this metric.

Moving to the rate metric, consider again the more general case for the GHZ state under any of the possible schemes. The first thing to notice is that while performing a minimization over all nodes for placing the coordination center, one can never actually reduce the maximum of the communications time while adding another path. This comes from the fact that in a tree, if after adding another path, this coordination center position changes, it must change to a place that still has a larger communications time, or else the previous position was not the one for the minimum to be attainable. From this it is very easy to see that adding any path with a probability $0 \leq p_{m:n} \leq 1$ and a waiting time $t_{m:n} > 0$ would result in either:

$$\begin{aligned} \xi = \frac{a}{2b} \mapsto \xi' &= \frac{a \cdot p_{m:n}}{2 \cdot \min_{s \in \mathcal{S}} \left\{ \max_{\tau \in \mathcal{J}} \{t_{s:\tau}\} \right\}} = \\ &= \begin{cases} \frac{a \cdot p_{m:n}}{2b} \\ \frac{a \cdot p_{m:n}}{2b'} \end{cases}, \text{ with } b' > b \end{aligned} \quad (\text{E3})$$

In either possible case the rate always decreases. This proves that both the fidelity metric and the rate metric for a GHZ state, under any of the possible schemes, is monotonic.

Appendix F: Label-Isotonicity

In this section we will focus on the properties of the algebras for trees in a GHZ state distribution under the star scheme, namely in determining they are label-isotone

with respect to every single algebra for routing. Starting with the fidelity metric. This metric has a correspondent algebra given by:

$f_{\text{GHZ}} : ([1/2; 1] \cup \{0\}, \geq, (1/2; 1), (0; 1)^3, 0, \oplus_{\text{GHZ}}, h)$
with $\oplus_{\text{GHZ}} : (0; 1)^3 \times (1/2; 1) \rightarrow (0; 1)^3$ given by:

$$(\{a, b, c\}, F_{m:n}) \mapsto \left\{ a \cdot \frac{1 + 2F_{m:n}}{3}, b \cdot \frac{2(1 - F_{m:n})}{3}, c \cdot \frac{4F_{m:n} - 1}{3} \right\} \quad (\text{F1})$$

and $h(\cdot)$ given by:

$$h(\{a, b, c\}) = \begin{cases} \frac{a+b+c}{2} & , \text{ if } \frac{a+b+c}{2} \geq 1/2 \\ 0 & , \text{ if } \frac{a+b+c}{2} < 1/2 \end{cases} \quad (\text{F2})$$

Consider a tree t with corresponding fidelity signature $\{a, b, c\}$ and two different paths σ_1, σ_2 such that $\sigma_1 \preceq \sigma_2$ in terms of fidelity, *i.e.* σ_1 has a fidelity given by $F_{m:n}^{(1)}$ and σ_2 has a fidelity given by $F_{m:n}^{(2)}$. Then:

$$\begin{aligned} F_{m:n}^{(1)} \geq F_{m:n}^{(2)} &\Rightarrow \\ \Rightarrow a \cdot \frac{1 + 2F_{m:n}^{(1)}}{3} + b \cdot \frac{2(1 - F_{m:n}^{(1)})}{3} + c \cdot \frac{4F_{m:n}^{(1)} - 1}{3} \\ &= \frac{a + 2b - c}{3} + \frac{2a - 2b + 4c}{3} \cdot F_{m:n}^{(1)} \\ &\geq \frac{a + 2b - c}{3} + \frac{2a - 2b + 4c}{3} \cdot F_{m:n}^{(2)}, \forall a, b, c \in (0, 1) \end{aligned} \quad (\text{F3})$$

Proving therefore the label-isotonicity of the fidelity of a GHZ state. As for the rate, the corresponding algebra for trees, under a star scheme, is given by:

$\xi_{\text{GHZ}} : (\mathbb{R}_0^+, \geq, (0, 1) \times \mathbb{R}^+, (0, 1) \times \mathbb{R}^+, 0, \oplus_{\xi}, g)$ with

$\oplus_{\xi} : ((0, 1) \times \mathbb{R}^+) \times ((0, 1) \times \mathbb{R}^+) \rightarrow (0, 1) \times \mathbb{R}^+$ given by:

$$(\{a, b\}, \{p_{m:n}, t_{m:n}\}) \mapsto \{a \cdot p_{m:n}, \max(b, t_{m:n})\} \quad (\text{F4})$$

and $g(\cdot)$ given by:

$$g(\{a, b\}) = \frac{a}{2b} \quad (\text{F5})$$

As one can see, this algebra actually depends on two parameters from each path: the probability of success and the communications time. For this reason, we have to guarantee that the algebra is label-isotone with respect to each parameter in order for *Proposition 1* to work. Starting with the probability of success, consider two paths with corresponding probabilities $p_{m:n}^{(1)}$ and $p_{m:n}^{(2)}$ such that:

$$\begin{aligned} p_{m:n}^{(1)} \geq p_{m:n}^{(2)} &\Rightarrow \\ \Rightarrow \frac{a \cdot p_{m:n}^{(1)}}{2b} &\geq \frac{a \cdot p_{m:n}^{(2)}}{2b}, \forall a \in (0, 1), \forall b \in \mathbb{R}^+ \end{aligned} \quad (\text{F6})$$

Moving to the communications time, consider two paths with corresponding communication times $t_{m:n}^{(1)}$ and $t_{m:n}^{(2)}$ such that:

$$\begin{aligned} t_{m:n}^{(1)} \leq t_{m:n}^{(2)} &\Rightarrow \\ \Rightarrow \frac{a}{2 \max(b, t_{m:n}^{(1)})} &\geq \frac{a}{2 \max(b, t_{m:n}^{(2)})}, \forall a \in (0, 1), \forall b \in \mathbb{R}^+ \end{aligned} \quad (\text{F7})$$

This guarantees that both metrics are label-isotonic with respect to the corresponding algebras for routing, allowing the dominance relation used for paths to be cohesive with the dominance relation used for trees and ensuring the optimality of our algorithm.